

T.M. Mukametkali, A.K. Aimukhanov, A.K. Zeinidenov*

Karaganda Buketov University, Scientific Center of nanotechnology and functional nanomaterials,
University str., 28, 100028 Karaganda, Kazakhstan

*Corresponding author's e-mail: a.k.zeinidenov@gmail.com

Phthalocyanine and metal phthalocyanine are hole transport buffer layers for perovskite solar cell fabrication

This approach allows you to more accurately evaluate the performance of solar panels and identify any problems or degradation in their operation. The LUMO value of mPc closer to the LUMO value of $\text{CH}_3\text{NH}_3\text{I}_3\text{PbCl}_x$ increased conversion energy and short circuit current density (J_{sc}), which reached a maximum value of 15.97 mA/cm² using the HTL layer of CuPc, and the open circuit voltage (V_{oc}) reached a maximum at 0.97 V. The change in J_{sc} corresponds to the fill factor (FF) change. The filling factor (FF) reached a maximum value of 67.35 % when using the HTL layer of CuPc and a minimum value (FF) of 54.23 % when using the HTL layer of H_2Pc . The lowest series resistance (R_1) and interface resistance (R_3) of 11.2 and 39.9 Ohms, respectively, were shown with the HTL layer of CuPc, Capacitive element CPE1 — 305 pF, Capacitive element CPE2 — 0.95 pF. CPE (Constant Phase Element) is an element used in equivalent circuits to describe the non-ideal dielectric properties of materials. The decrease in CPE1 may indicate a decrease in the heterogeneity of the dielectric properties of the perovskite material after coating with different HTL mPc layers. This may be due to changes in structure or mutual actions between layers as a result of exposure to differences in energy levels.

Keywords: Perovskite solar cells, hole transport layers, metalphthalocyanine, absorption spectra, photovoltaic properties, electrical impedance spectroscopy, ion migration.

Introduction

Phthalocyanine molecules have attracted widespread attention due to their outstanding thermal and chemical stability and other promising properties. This class of molecules is actively studied in various technologically important fields such as magnetism, sensing, and optoelectronics due to the diverse chemical composition and aromatic structure of the molecule. MPc macrocycles (M = Co, Cu, Ni, or Fe) have fourfold symmetry and are typically adsorbed with their molecular plane parallel to the surface on metal surfaces. In addition, MPc is often used as a protective coating for the photoactive perovskite layer, and its high thermal and chemical stability can be extremely beneficial for the operation of perovskite salt solar cells (PSCs) [1–4].

Perovskite solar cells have several advantages, such as high open circuit voltage and high conversion efficiency, due to a wide optical absorption spectrum. A typical perovskite solar cell design includes titanium oxide for electron transfer, a $\text{CH}_3\text{NH}_3\text{PbI}_3$ perovskite crystal as the photoactive layer, and a N'-octakis(4-methoxyphenyl)-9,9'-spirobi[9H-fluorene]-2,2',7'-tetramine (spiro-OMeTAD) for hole transfer. However, to improve the photovoltaic properties and chemical stability, there was a need to develop materials that could replace spiro-OMeTAD as the hole transport layer. In recent years, phthalocyanine complexes have begun to be used as organic semiconductors by modifying their molecular structure, including central metal chemical groups and electronic structures [5–7]. Phthalocyanine plays an important role in improving semiconductivity, charge carrier mobility, recombination-free carrier diffusion, and conversion efficiency.

However, complex synthesis processes and difficulties in purifying Spiro-OMeTAD lead to increased production costs. Moreover, due to the primary structure of Spiro-OMeTAD, all significant conversion efficiencies were achieved by adding dopants and impurities, which further increases the overall cost of the devices and reduces their stability. Due to this, significant efforts have been made to develop more affordable, impurity-free alternatives using simpler syntheses. Various design strategies and various types of impurity-free hole transport materials (HTM) have been developed. Our group first reported the use of cuprophthalocyanine (CuPc) with MoO_3 as a hybrid HTM, achieving an efficiency of 8.12 %.

Metal phthalocyanines (MPcs) offer exciting potential as p-type semiconductor materials for use as hole transport layer (HTL) materials in perovskite solar cells (PSCs). MPcs boast high electrical conductivity, catalytic activity, and exceptional chemical and thermal stability. Furthermore, the alignment of the valence band maximum (VBM) and conduction band minimum (CBM) levels of the MPC with the energy levels of the perovskite and counter electrodes ensures efficient device operation [8, 9]. This strong compatibility be-

tween the MPC and other layers of the perovskite solar cell significantly enhances its performance and stability.

Research has shown that direct contact between perovskite layers and MoO_3 causes an undesirable chemical reaction. P. Schulz and his team investigated the chemical and electronic structure of the $\text{MoO}_3/\text{MAPbI}_3$ interface. They discovered that direct contact of perovskite with MoO_3 leads to the reduction of MoO_3 to MoO_2 . The alignment of energy levels at the perovskite/ MoO_2 interface is not favorable for hole extraction. These findings were confirmed by F. Schulz and his colleagues. They studied the chemical reaction occurring at the boundary of the $\text{CH}_3\text{NH}_3\text{PbCl}_x\text{I}_{3-x}$ and MoO_3 layer. Changing the valency of Mo in MoO_3 from Mo^{6+} to Mo^{4+} led to an increase in the concentration of MoO_2 . The oxidation of Pb^{2+} to Pb^{4+} or the oxidation of $2\Gamma^-$ to Γ^{2-} is accompanied by a change in the valence of Mo from Mo^{6+} to Mo^{4+} [10]. This leads to the formation of regions with a high density of defects at the interface, which become recombination centers and reduce the performance of the perovskite solar cells.

To solve this problem, we applied a metal phthalocyanine (MPC) layer as an HTL interlayer. MPC has excellent charge transfer properties and can effectively act as an HTL. Selection and optimization of HTL layers are challenging tasks in the research and development of perovskite solar cells (PSCs). It is necessary to achieve a balance between electrical conductivity, hole permeability, stability, adhesion to the perovskite layer, and other factors to achieve high efficiency and stability of solar cells [11–14].

In this study, we propose adding an extra layer of phthalocyanine and its metal complexes between the perovskite and the hole-conducting MoO_x layer in order to enhance the efficiency and stability of perovskite solar cells (PSCs). Our plan is to investigate and optimize the composition and structure of phthalocyanine and its metal complexes, as well as various methods for their integration into perovskite material. Additionally, we intend to examine how phthalocyanine nanostructures and their metal complexes affect the efficiency of charge carrier transport in a perovskite solar cell.

Materials and Methods

Sample preparation and deposition process

The fabrication process of the perovskite solar cells (PSCs) involves several steps, including the preparation of substrates, deposition of the electron transport layer (ETL) and perovskite layer, and deposition of the hole transport layer (HTL) and electrode layers.

Substrate Preparation:

Glass substrates coated with a fluorine-doped tin oxide (FTO) layer are cleaned thoroughly using acetone, hot deionized water, and 2-propanol. Subsequently, UV-ozone treatment is performed.

Deposition of Electron Transport Layer (ETL):

A titanium dioxide (TiO_2) sol-gel solution is prepared by mixing titanium VI isopropoxide (TTIP), acetic acid, deionized water, isopropanol, and nitric acid. The solution is spin-coated onto the FTO-coated glass substrates and annealed at 500°C to obtain a crystalline TiO_2 layer.

Deposition of Perovskite Layer:

A solution containing methylammonium iodide (MAI) and lead chloride (PbCl_2) dissolved in N,N-Dimethylformamide (DMF) solvent is prepared. This perovskite solution is spin-coated onto the TiO_2 surface at various speeds and annealed at 90°C to form a crystalline perovskite layer.

Deposition of Hole Transport Layer (HTL): Metal phthalocyanine (MPC) is deposited as the HTL on the perovskite surface via thermal evaporation. Subsequently, a layer of molybdenum oxide (MoO_x) is thermally evaporated on top of the MPC layer.

Deposition of Electrode Layers: An anode layer of silver (Ag) is thermally evaporated onto the MoO_x layer to complete the device structure. Throughout the fabrication process, precautions are taken to perform all steps in a glove box filled with nitrogen to minimize exposure to moisture and oxygen, which could degrade the performance of the PSCs.

The structural formulas of MPC, MAI, and PbCl_2 , as well as a diagram illustrating the fabrication steps of the perovskite solar cells (PSCs) and the structure of PSCs with energy diagrams of functional layers, are provided in Figure 1 for reference.

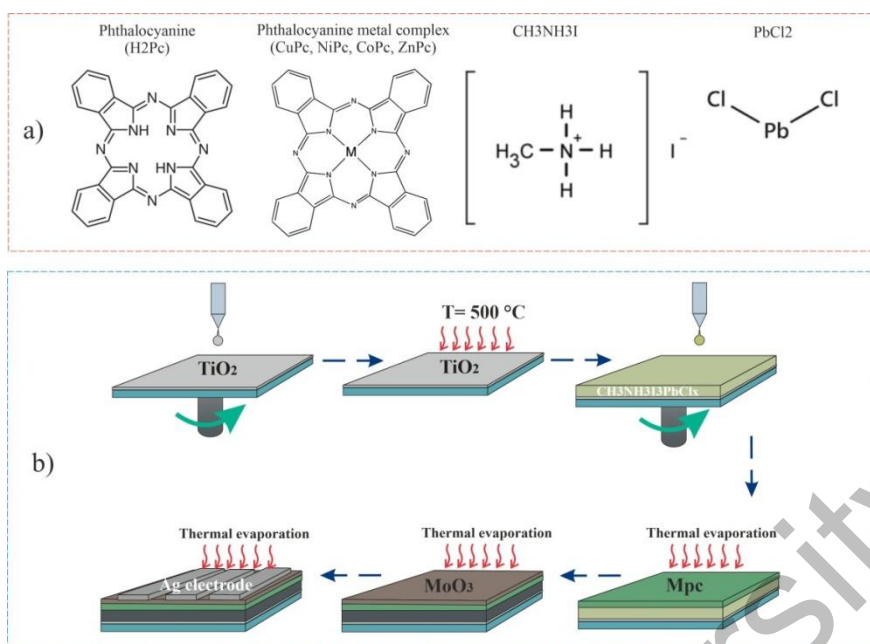


Figure 1. Structural formulas (a), a scheme of perovskite solar cell fabrication steps (b)

Analysis methods

The surface topography and thickness of the samples were probed using a JEOL JSPM-5400 atomic force microscope (AFM). The AFM data were processed using Gwyddion Data-Processing Software, a modular program for SPM (scanning probe microscopy) data visualization and analysis. To measure the local current distribution, an AFM Solver P47 (NT-MDT) was utilized. During current measurements, a voltage was applied to the sample, while the conductive probe covered with a gold film was grounded. The surface topography and root mean square (rms) roughness were measured in the semi-contact mode using an NSC14 probe from Micromash, while the current was measured in the contact mode using a CSC37/Au probe from Micromash.

The absorption spectra of the samples were measured using an AvaSpec-ULS2048CL-EVO spectrometer (Avantes). A combined deuterium-halogen light source AvaLight-DHc (Avantes) with an optical range of 200–2500 nm was employed as the light source. For thermal deposition, the CY-1700x-spc-2 vacuum sputtering unit (Zhengzhou CY Scientific Instruments Co., Ltd) was utilized.

The impedance spectra were measured using a P45X potentiostat-galvanostat with an FRA (frequency response analyzer) module. The current-voltage (I-V) characteristics of solar devices were measured using a PVIV-1A I-V Test Station under light illumination from a Sol3A Class AAA Solar Simulator (Newport).

Results and Discussion

Structural analysis of the prepared films

Figure 2 presents AFM images of the HTL layer's surface composed of various phthalocyanines and MoO₃, created through vacuum thermal deposition. The figure reveals that the HTL layer's surface morphology, when using different metal phthalocyanines and MoO₃, exhibits a granular structure with distinct boundaries. Given that the particle size is roughly equivalent to the film's thickness, it's evident that these films possess a greater number of defects and pores compared to others. For instance, CoPc films with a 250 nm thickness have an average particle size of 230 nm, suggesting a substantial amount of defects and pores. Conversely, CuPc films at 230 nm thickness have an average particle size of 110.9 nm, nearly half the film's thickness, indicating fewer defects and pores. Determining the average particle size in H₂Pc and MoO₃ films is challenging, as such structures' emergence could be attributed to the glass substrate's surface characteristics.

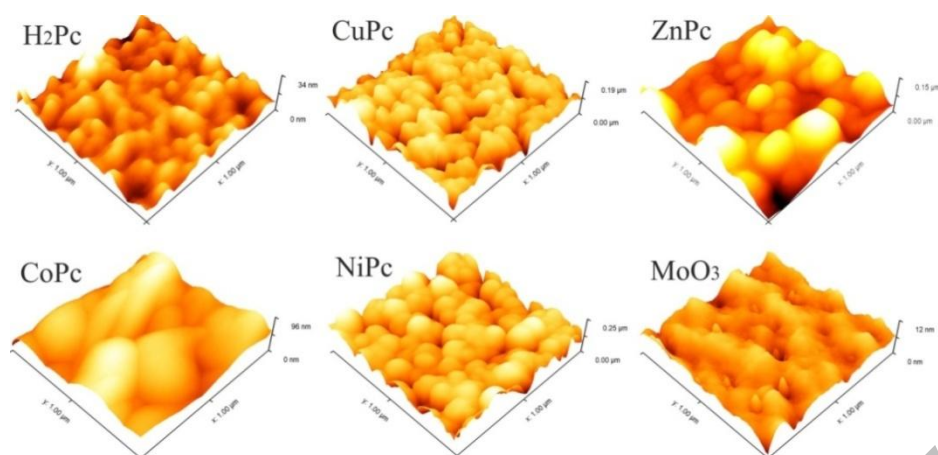


Figure 2. AFM images of hole-transport layers phthalocyanine (a) and molybdenum oxide

Table 1

Phthalocyanine and MoO₃ film roughness and particle size

Sample name	Thickness, nm	R_a , nm	d_{avg} , nm
H ₂ Pc	220	2.75	undetermined
CuPc	230	19.88	110
ZnPc	250	19.5	200
CoPc	250	9.37	230
NiPc	270	27.28	162
MoO ₃	60-70	1.11	undetermined

Optical properties

Figure 3 shows the absorption spectra of metal and nonmetal phthalocyanine nanostructures. The absorption spectra show two very intense bands in the region of 300–400 nm (B-band), which correspond to mixed π - π^* and n - π transitions $a_{2u} \rightarrow 2e_g$ and $b_{2u} \rightarrow 2e_g$, as well as an absorption band in the region of 550–750 nm (Q-range), which corresponds to the π - π^* transition $a_{1u} \rightarrow 2e_g$ [15]. The absorption spectrum of a vacuum-deposited CuPc film (Fig. 3, curve 1) in the Soret region has a maximum at $\lambda=326$ nm, and in the Q-range, two bands are observed with maxima at $\lambda=616$ nm and $\lambda=692$ nm. The characteristic splitting of the absorption of nanostructures in the Q-range into two peaks is associated with Davydov splitting [16].

Understanding the optical absorption spectra of thin films is crucial for revealing the band structure and energy gap of both crystalline and amorphous structures. The substitution of metal ions in phthalocyanine, as well as the type of metal ions, can significantly alter the absorption and the position of the bands in these regions. Phthalocyanine films display distinct absorption spectra in the B-range around 300–350 nm and in the Q-range 550–650 nm, which are influenced by the metal complex [10, 16].

The graph in Figure 3 illustrates the spectral absorption distributions of thin PC films (1–3) within the 300–900 nm wavelength range. Notably, the films exhibited over 75 % transparency in the 400–500 nm and above 750 nm wavelength regions. It is worth mentioning that metal-free phthalocyanine (H₂Pc) and nickel phthalocyanine show a pronounced Q-band absorption region around 599 nm. Conversely, metal phthalocyanine thin films (CuPc and ZnPc) display a red-shift in these regions. Specifically, absorption peaks were observed at 321, 599, and 686 nm for H₂Pc, 321, 602, and 693 nm for CuPc, 330, 602, and 697 nm for ZnPc, 318, 600, and 693 nm for CoPc, and 327, 599, and 681 nm for NiPc.

The Tauc plot [17] was used to calculate the optical band gap of MPc films by plotting the dependence of $(\alpha h\nu)^2$ on photon energy for thin films of H₂Pc, CuPc, ZnPc, CoPc, and NiPc (Fig. 3b). It was found that the bandgap for metal-free thin films was approximately 1.63 eV. Moreover, the corresponding energies for CuPc, ZnPc, CoPc, and NiPc thin films were 1.60, 1.61, 1.65, and 1.67 eV, respectively, indicating a slight difference.

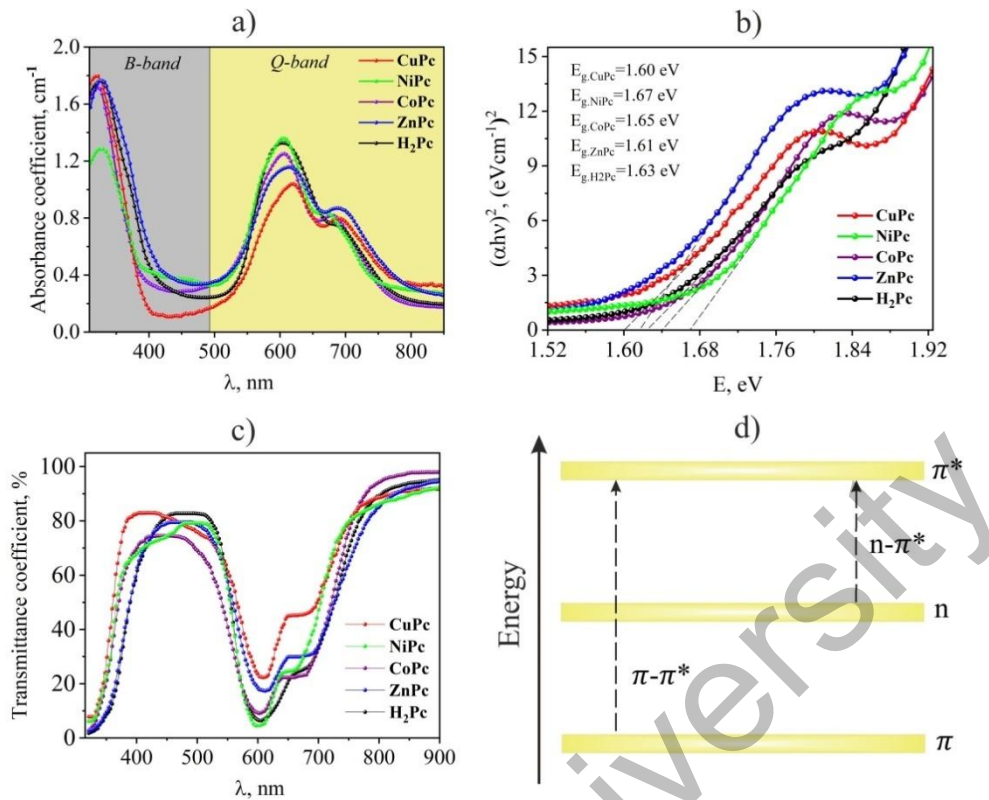


Figure 3. Phthalocyanine films absorbance coefficient (a), optical band gap (b), transmittance coefficient (c) and diagram of electronic transitions (d)

Table 2

Absorbance coefficient, optical bandgap, and transmittance coefficient

Sample name	B-band		Q-band		Band gap, eV	Transmittance (%) in λ=700 nm
	λ max, nm	FWHM, nm	λ max, nm	FWHM, nm		
H ₂ Pc	320.89	103.41	599.33	83.05	1.63	50
			686.49	107.49		
CuPc	321.04	79.21	602.21	85.06	1.60	70
			693.14	115.19		
ZnPc	329.70	90.02	601.70	88.11	1.61	50
			697.18	104.84		
CoPc	317.91	76.03	599.96	87.06	1.65	50
			692.67	73.69		
NiPc	327.23	66.84	598.71	75.92	1.67	70
			680.85	77.51		

Photoelectrical and Electrical Impedance Spectroscopy characterizations

From Figure 4 and Table 3, it can be seen that the lowest LUMO value for CuPc is -5.2 eV, which is closer to the LUMO of the photoactive layer, resulting in improved photovoltaic performance. The device with the HTL CuPc layer showed the highest performance with a power conversion efficiency (PCE) of 10.28 %. At the highest LUMO of -5.1 and -5.0 eV, the photovoltaic performance of PSCs showed lower values compared to devices based on more positive LUMOs.

Decreasing the LUMO value of Pc closer to the LUMO value of $\text{CH}_3\text{NH}_3\text{I}_3\text{PbCl}_x$ increased conversion energy and short circuit current density (J_{sc}), which reached a maximum value of 15.97 mA/cm² using the HTL layer of CuPc, and the open circuit voltage (V_{oc}) reached a maximum at 0.97 V. The change in J_{sc} corresponds to the fill factor (FF) change. The filling factor (FF) reached a maximum value of 67.35 % when using the HTL layer of CuPc and a minimum value (FF) of 54.23 % when using the HTL layer of H₂Pc.

All PSC functional layers, except the different HTL materials, were deposited under the same conditions, so the observed differences in photovoltaic performance are mainly due to the properties of the phthalocyanine HTL and the phthalocyanine/perovskite interface. The differences in the change in fill factor (FF) and hence J_{sc} are largely due to the change in HTL mPc conductivity caused by the change in HTL mPc. J_{sc} is also affected by the mPc/perovskite interface. It is well known that the compatibility of LUMO energy levels for Pc and LUMO for $CH_3NH_3I_3PbCl_x$ reduces its resistivity and increases the conductivity of the film. Therefore, matching the energy levels should lead to an increase in its conductivity, and in the device, this should improve the fill factor (FF) and increase J_{sc} .

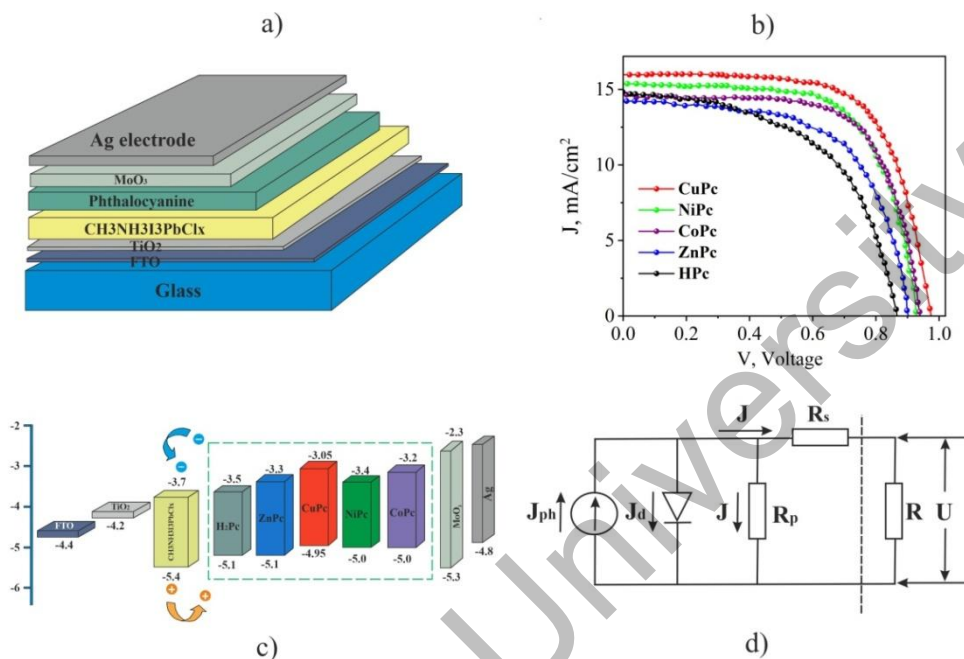


Figure 4. The structure of the device (a), current-voltage characteristics (b), energy diagram (c), and diagram of a single-diode model of the electrical characteristics of IOSC (d)

Table 3

Photovoltaic performance of perovskite solar cells

PSC's HTL	J_{sc} mA/cm ²	V_{oc} V	J_{max} mA/cm ²	V_{max} V	FF %	η %
CuPc	15.97	0.97	13.01	0.79	67.35	10.28
NiPc	15.38	0.94	12.47	0.75	66.39	9.35
CoPc	14.59	0.93	11.98	0.77	65.26	9.22
ZnPc	14.22	0.90	11.16	0.71	61.91	7.92
H ₂ Pc	14.76	0.87	10.88	0.64	54.23	6.96

To gain a detailed understanding of how the mPc HTL layer affects charge carrier transport mechanisms, we conducted impedance spectroscopy on perovskite solar cells. The impedance spectra were analyzed and fitted using the equivalent electrical circuit depicted in Figure 5a.

EIS is a non-destructive electrical characterization technique used to study the bulk and interface electrochemical dynamics of various materials with both electronic and ionic behavior, such as solar cells, various electrochemical electrodes, batteries, and fuel cells. EIS measures the resistive and capacitive behavior of an electrochemical system by applying an alternating current (AC) potential at different frequencies and measuring the AC response through the cell. EIS can be used in combination with light illumination to characterize solar cells under operating conditions. Various physical processes occurring in the device will manifest themselves in EIS responses at different characteristic frequencies.

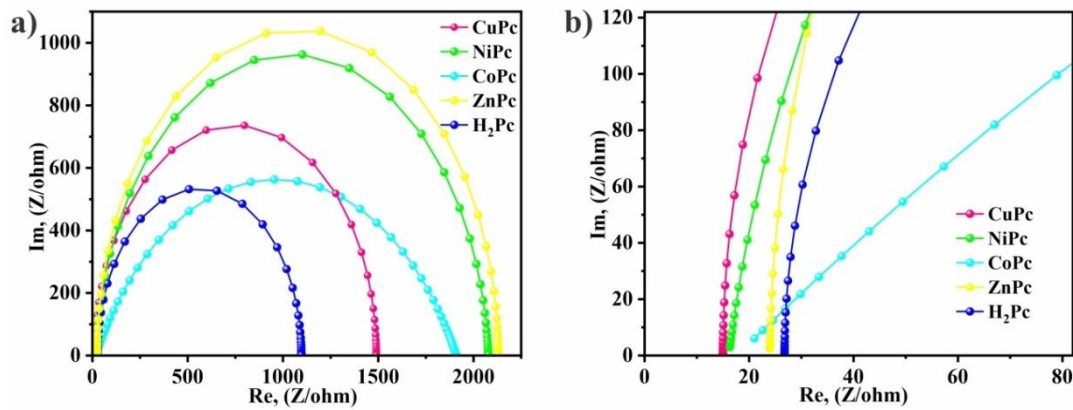


Figure 5. Nyquist impedance curves and equivalent circuit diagrams (insert) (a), and increased high-frequency region curves (b) for perovskite solar cells

To interpret the EIS, the dual time constant equivalent circuit model proposed by Garcia-Belmonte and colleagues [18, 19] is used. The circuit is a combination of a series of external resistance (R_1), including contact resistance, wire resistance, and electrode surface resistance, two non-ideal capacitive elements called constant phase elements (CPE_1 and CPE_2), and two resistive elements (R_2 and R_3). The constant phase element (CPE) impedance is given by:

$$Z_{pce} = \frac{1}{T(j\omega)^p} \quad (1)$$

T is a constant with unit $F \text{ cm}^{-2}$, and P is related to the purity angle. The capacitive element CPE_1 represents a non-ideal geometric capacitance and is related to the dielectric response of the perovskite layer, which dominates the capacitive response in the high-frequency region ($> 1 \text{ kHz}$) of the spectra. The second capacitive element CPE_2 is a low-frequency characteristic ($< 1 \text{ Hz}$) related to the accumulation of surface charge at the solar cell interfaces. The resistance R_2 is related to CPE_1 and is related to the charge transfer resistance of the bulk perovskite. This is also influenced by the low-frequency transport resistance R_3 is associated with many processes such as surface resistance, storage resistance at interfaces, as well as slow processes such as ion diffusion and resistance to trap-mediated charge recombination in the bulk.

So, it is possible to extract the parameters of the equivalent circuit under 8 mW/cm^2 LED illumination (solar simulator) from the provided experiment. These are the parameters:

The lowest series resistance (R_1) and interface resistance (R_3) of 11.2 and 39.9 Ohms, respectively, was shown with the HTL layer of CuPc, Capacitive element CPE_1 — 305 pF, Capacitive element CPE_2 — 0.95 pF. CPE (Constant Phase Element) is an element used in equivalent circuits to describe the non-ideal dielectric properties of materials. The decrease in CPE_1 may indicate a decrease in the inhomogeneity of the dielectric properties of the perovskite material after coating with different HTL mPc layers. This may be due to changes in structure or mutual actions between layers as a result of exposure to differences in energy levels.

These changes could be significant for optimizing the performance of perovskite solar cells and other devices utilizing perovskite materials. This is because the dielectric properties of the material can impact its electrochemical stability, energy conversion efficiency, and other important performance parameters. The increase in CPE_2 may be attributed to the accumulation of ions and electrons at the interfaces as shown in Table 4.

Table 4

The value of charge transport parameters of perovskite solar cells

PSC's HTL	R_1 , Ohm	R_2 , Ohm	R_3 , Ohm	p_1	n_1	p_2	n_2
CuPc	11.2	1478.8	39.9	$3.05 \cdot 10^{-10}$	1	$9.5 \cdot 10^{-13}$	0.03
NiPc	16.1	1642.9	428.6	$1.4 \cdot 10^{-10}$	0.96	$7.4 \cdot 10^{-7}$	0.72
CoPc	24.9	1723.4	339.3	$7.5 \cdot 10^{-11}$	1	$6.7 \cdot 10^{-10}$	0.86
ZnPc	24.0	1909.2	234.5	$7.3 \cdot 10^{-11}$	0.99	$4.9 \cdot 10^{-4}$	0.32
H ₂ Pc	27.47	986.6	110.9	$2.7 \cdot 10^{-10}$	1	$1.3 \cdot 10^{-12}$	0.11

Conclusions

The decrease in CPE_1 may indeed indicate a decrease in the heterogeneity of the dielectric properties of the perovskite material after coating with various layers such as HTL mPc. When coated with different layers, changes can occur in the structure of the perovskite material, as well as interactions between these layers, for example, as a result of differences in energy levels. These changes can affect the dielectric properties of the material, including its heterogeneity. Such analysis helps to understand what processes occur at the interface level and how they affect the electrical characteristics of perovskite solar cells.

The lowest series resistance (R_1) and interface resistance (R_3) of 11.2 and 39.9 Ohms, respectively, was shown with the HTL layer of CuPc, Capacitive element CPE_1 — 305 pF, Capacitive element CPE_2 — 0.95 pF. CPE (Constant Phase Element) is an element used in equivalent circuits to describe the non-ideal dielectric properties of materials. The decrease in CPE_1 may indicate a decrease in the inhomogeneity of the dielectric properties of the perovskite material after coating with different HTL mPc layers. This may be due to changes in structure or mutual actions between layers as a result of exposure to differences in energy levels [10, 20].

Such changes could be important for optimizing the performance of perovskite solar cells and other devices using perovskite materials since the dielectric properties of the material can affect its electrochemical stability, energy conversion efficiency, and other key performance parameters. The increase in CPE_2 may be due to the accumulation of ions and electrons at the interfaces.

Acknowledgments

This research is funded by the Science Committee of the Ministry of Science and Higher Education of the Republic of Kazakhstan (Grant No. AP19576784).

References

- 1 Wu, X. (2023). Realizing 23.9 % Flexible Perovskite Solar Cells via Alleviating the Residual Strain Induced by Delayed Heat Transfer. *ACS Energy Letters*, 8 (9), 3750–3759. <https://doi.org/10.1021/acsenergylett.3c01167>
- 2 Petraki, F., Papaefthimiou, V., & Kennou, S. (2005). A study of the Ni-phthalocyanine/gold interface using x-ray and ultraviolet photoelectron spectroscopies. *J. Phys., Conf. Ser.*, 10, 135. <https://doi.org/10.1088/1742-6596/10/1/033>
- 3 Zhou, Q., Liu, Z.-F., Marks, T.J., & Darancet, P. (2021). Electronic Structure of Metallophthalocyanines, MPc (M = Fe, Co, Ni, Cu, Zn, Mg) and Fluorinated MPc. *The Journal of Physical Chemistry A*, 125(19), 4055–4061. <https://doi.org/10.1021/acs.jpca.0c10766>
- 4 Zavgorodniy, A., Aimukhanov, A., Zeinidenov, A., & Akhatova, Zh. (2019). Study of the effect of an external magnetic field on the photoelectric properties of a copper phthalocyanine film. *Bulletin of the University of Karaganda-Physics*, 2019 (93) 1, 18–25. <https://doi.org/10.31489/2019Ph1/18-25>
- 5 Tağman, İ., Özçeşmeci, M., Gümrükçi, S., & Sorar, İ. (2021). Spectroscopic, electrochemical and optical properties of non-peripherally (2,2-dimethyl-1,3-dioxolan-4-yl)methoxy groups substituted metal-free and metallophthalocyanines, *Journal of Molecular Structure*, 1245, 131045, ISSN 0022-2860. <https://doi.org/10.1016/j.molstruc.2021.131045>
- 6 Park, N.G., Grätzel, M., Miyasaka, T. et al. (2016). Towards stable and commercially available perovskite solar cells. *Nat Energy*, 1, 16152. <https://doi.org/10.1038/nenergy.2016.152>
- 7 Grätzel, M., (2014). The light and shade of perovskite solar cells. *Nature Mater.*, 13, 838–842. <https://doi.org/10.1038/nmat4065>
- 8 Tazhibayev, S.K., Beisembekov, M.K., Rozhkova, X.S., Zhakanova, A.M., Aimukhanov, A.K., Makhabayeva, A.T., & Zeinidenov, A.K. (2023). Impact of the thickness of phthalocyanine films and its metal complexes on optical and electrical properties. *Bulletin of the University of Karaganda-Physics*, 112 (4), 14–22. <https://doi.org/10.31489/2023PH4/14-22>
- 9 Yang J.P., Meissner, M., Yamaguchi, T., Zhang, X.Y., Ueba, T., Cheng, L.W., Ideta, S., Tanaka, K., Zeng, X.H., Ueno, N., & Kera, S. (2018). Band dispersion and hole effective mass of methylammonium lead iodide perovskite, *Solar RRL*, 2. <https://doi.org/10.1002/solr.201800132>
- 10 Schulz, P., Tjepelt, J.O., Christians, J.A., Levine, I., Edri, E., Sanehira, E.M., Hodes, G., Cahen, D., & Kahn, A. (2016). High-Work-Function Molybdenum Oxide Hole Extraction Contacts in Hybrid Organic–Inorganic Perovskite Solar Cells. *ACS Appl. Mater. Interfaces*, 8, 46, 31491–31499. <https://doi.org/10.1021/acsami.6b10898>
- 11 Atsushi Suzuki, Hiroki Okumura, Yasuhiro Yamasaki, & Takeo Oku. Fabrication and characterization of perovskite type solar cells using phthalocyanine complexes. <https://doi.org/10.1016/j.apsusc.2019.05.305>
- 12 Suzuki, A., & Oku, T. (2017). Electronic structures, and optical and magnetic properties of quadruple-decker phthalocyanine, *Magnetochemistry*, 3. <https://doi.org/10.3390/magnetochemistry3020021>.

- 13 Guo, J.J., Bai, Z.C., Meng, X.F., Sun, M.M., Song, J.H., Shen, Z.S., Ma, N., Chen, Z.L., & Zhang, F. (2017). Novel dopant-free metallophthalocyanines based hole transporting materials for perovskite solar cells: the effect of core metal on photovoltaic performance, *Sol. Energy*, 155, 121–129. <https://doi.org/10.1016/j.solener.2017.05.089>.
- 14 Suzuki, A., Ueda, H., Okada, Y., Ohishi, Y., Yamasaki, Y., & Oku, T. (2017). Effects of metal phthalocyanines as hole-transporting layers of perovskite-based solar cells, *Chemical and Materials Engineering* 5, 34–42. <https://doi.org/10.13189/cme.2017.050203>.
- 15 Cao, G., Lia, L., Guana, M., Zhao, J., Li, Y., & Zeng, Y. (2011). Stable organic solar cells employing MoO₃-doped copper phthalocyanine as buffer layer, *Applied Surface Science*, 257, 9382–9385. <https://doi.org/10.1016/j.apsusc.2011.05.120>
- 16 Ghosh, P.N. (1976). Davydov splitting and multipole interactions. *Solid State Communications*, 19, I. 7, 639-642, ISSN 0038-1098, [https://doi.org/10.1016/0038-1098\(76\)91093-0](https://doi.org/10.1016/0038-1098(76)91093-0).
- 17 Jubu, P.R., Obaseki, O.S., Nathan-Abutu, A., Yam, F.K., Yusof, Y., & Ochang, M.B. (2022). Dispensability of the conventional Tauc's plot for accurate bandgap determination from UV–vis optical diffuse reflectance data. *Results in Optics*, 9, 100273, ISSN 2666-9501. <https://doi.org/10.1016/j.rio.2022.100273>.
- 18 Zarazua, I., Han, G., Boix, P.P., Mhaisalkar, S., Fabregat-Santiago, F., Mora-Seró, I., Bisquert, J., & Garcia-Belmonte, G. (2016). Surface recombination and collection efficiency in perovskite solar cells from impedance analysis *J. Phys. Chem. Lett.*, 7, 5105. <https://doi.org/10.1021/acs.jpcclett.6b02193>
- 19 Zarazúa, I., Sidhik, S., López-Luke, T., Esparza, D., De la Rosa, E., Reyes-Gomez, J., Mora-Seró, I., & Garcia-Belmonte, G. (2017). Operating Mechanisms of Mesoscopic Perovskite Solar Cells through Impedance Spectroscopy and J-V Modeling. *J. Phys. Chem. Lett.*, 8, 6073. <https://doi.org/10.1021/acs.jpcclett.7b02848>
- 20 Kayumova, A., Savilov, S., Zhanbirbayeva, P., Baltabekov, A., Dzhakupova, M., & Serikov, T. (2023). Effect of TNR/Ag/rGO film area on its photocatalytic activity. *Bulletin of the University of Karaganda-Physics*, 2023(112)4, 6–13. <https://doi.org/10.31489/2023ph4/6-13>

Т.М. Мұқаметқали, А.К. Аймуханов, А.К. Зейниденов

Фталоцианин және металл фталоцианин кемтік тасымалдаушы буферлік қабаттарын перовскит күн батареяларын өндіруге пайдалану

Бұл тәсіл күн батареяларының өнімділігін дәлірек бағалауға және олардың жұмысындағы кез келген проблемаларды немесе деградацияны анықтауға мүмкіндік береді. Фото активті қабат CH₃NH₃I₃PbCl_x LUMO мәніне жақын кемтік тасымалдаушы mPc LUMO мәні түрлендіру энергиясын және қысқа тұйықталу ток тығыздығын (J_{sc}) арттырды, ол CuPc кемтік тасымалдау қабатын пайдаланып 15,97 мА/см² максималды мәнге жетті және ашық тізбек кернеуі (V_{oc}) максимум 0,97 В-қа жетті. J_{sc} өзгерісі толтыру коэффициентінің (FF) өзгеруіне сәйкес келеді. Толтыру коэффициенті (FF) CuPc НТЛ қабатын пайдаланған кезде ең жоғары мәнге 67,35 % және H₂Pc НТЛ қабатын пайдаланған кезде ең төменгі мәнге (FF) 54,23 % жетеді. Ең төменгі сериялық кедергі (R₁) және интерфейсі кедергісі (R₃) сәйкесінше 11,2 және 39,9 Ом CuPc НТЛ қабатымен, SPE₁ сыйымдылық элементі — 305 пФ, SPE₂ сыйымдылық элементі — 0,95 пФ көрсетілді. SPE (тұрақты фазалық элемент) — материалдардың идеалды емес диэлектрлік қасиеттерін сипаттау үшін эквивалентті тізбектерде қолданылатын элемент. SPE₁ төмендеуі әртүрлі НТЛ mPc қабаттарымен қапталғаннан кейін перовскит материалының диэлектрлік қасиеттерінің гетерогенділігінің төмендеуін көрсетуі мүмкін. Бұл құрылымның өзгеруіне немесе энергия деңгейлеріндегі айырмашылықтардың әсерінен қабаттар арасындағы өзара әрекеттерге байланысты болуы мүмкін.

Кілт сөздер: перовскитті күн батареялары, өткізгіштік кемтігі бар қабат, металлфталоцианин, жұтылу спектрлері, фотоэлектрлік қасиеттері, импеданс спектроскопиясы, иондардың кезуі.

Т.М. Мұқаметқали, А.К. Аймуханов, А.К. Зейниденов

Перовскитные солнечные элементы с использованием фталоцианина и его металлокомплексов в качестве слоя с дырочной проводимостью

Указанный в работе подход позволяет более точно оценить работу солнечных панелей и выявить любые проблемы или деградацию в их работе. Уменьшение значения LUMO для mPc ближе к значению LUMO для CH₃NH₃I₃PbCl_x привело к увеличению энергии переобразования и плотности тока короткого замыкания (J_{sc}), которая достигла максимального значения в 15,97 мА/см² при использовании НТЛ слоя CuPc, а напряжение холостого хода (V_{oc}) достигло максимума в 0,97 В. Изменение J_{sc} соответствует изменению коэффициента заполнения (FF). Коэффициент заполнения (FF) достиг максимального значения в 67,35 % при применении НТЛ слоя CuPc и минимального значения в 54,23 % при использовании НТЛ слоя H₂Pc. Самое низкое последовательное

сопротивление (R_1) и сопротивление интерфейса (R_3) составили 11,2 и 39,9 Ом соответственно, показав лучший результат при использовании HTL слоя CuPc. Емкостные элементы — CPE_1 -305 пФ и CPE_2 -0,95 пФ. CPE (Constant Phase Element) является элементом, используемым в эквивалентных схемах, для описания неидеальных диэлектрических свойств материалов. Уменьшение CPE_1 может указывать на сокращение неоднородности диэлектрических свойств перовскитного материала после покрытия различными HTL слоями mPc. Это может быть связано с изменениями в структуре или взаимодействием между слоями из-за разницы в энергетических уровнях.

Ключевые слова: перовскитные солнечные элементы, слой с дырочной проводимостью, металлофталониан, спектры поглощения, фотоэлектрические свойства, импедансная спектроскопия, миграция ионов.

Information about the authors

Mukametkali Toktarbek — Master of physics, Doctoral student of the Department of Radiophysics and Electronics, Researcher, Karaganda Buketov University, Scientific Center of Nanotechnology and Functional Nanomaterials, Karaganda, Kazakhstan; e-mail: tmk625@mail.ru; ORCID: 0000-0003-2685-2976

Zeinidenov Assylbek — PhD, Associate professor, Dean of the Physics and Technology Faculty, Head of Scientific Center for Nanotechnology and Functional Nanomaterials, Karaganda Buketov University, Karaganda, Kazakhstan; e-mail: asyl-zeinidenov@mail.ru ORCID: 0000-0001-9780-5072

Aimukhanov Aitbek — Candidate of physical and mathematical sciences, Associate professor, Professor of the Department of Radiophysics and Electronics, Leading Researcher, Karaganda Buketov University, Scientific Center for Nanotechnology and Functional Nanomaterials, Karaganda, Kazakhstan; e-mail: a_k_aitbek@mail.ru ORCID: 0000-0002-4384-5164